Article (refereed) - postprint

Fleischer, Katrin; Rammig, Anja; De Kauwe, Martin G.; Walker, Anthony P.; Domingues, Tomas F.; Fuchslueger, Lucia; Garcia, Sabrina; Goll, Daniel S.; Grandis, Adriana; Jiang, Mingkai; Haverd, Vanessa; Hofhansl, Florian; Holm, Jennifer A.; Kruijt, Bart; Leung, Felix; Medlyn, Belinda E.; Mercado, Lina M.; Norby, Richard J.; Pak, Bernard; von Randow, Celso; Quesada, Carlos A.; Schaap, Karst J.; Valverde-Barrantes, Oscar J.; Wang, Ying-Ping; Yang, Xiaojuan; Zaehle, Sönke; Zhu, Qing; Lapola, David M.. 2019. **Amazon forest response to CO2 fertilization dependent on plant phosphorus acquisition.** *Nature Geoscience*, 12 (9). 736-741.
https://doi.org/10.1038/s41561-019-0404-9

Title:

Future CO_2 fertilization of the Amazon forest hinges on plant phosphorus use and acquisition

Author list:

K. Fleischer*, *Land Surface–Atmosphere Interactions, Technical University of Munich, Germany*
A. Rammig, *Land Surface–Atmosphere Interactions, Technical University of Munich, Germany*
M. G. De Kauwe, *University of New South Wales, Australia*
A.P. Walker, *Oak Ridge National Laboratory, United States*
T. F. Domingues, *University of São Paulo, Brazil*
L. Fuchslueger, *University of Antwerp, Belgium*
S. Garcia, *National Institute of Amazonian Research, Brazil*
D. Goll, *LSCE, France*
A. Grandis, *University of São Paulo, Brazil*
M. Jiang, *Western Sydney University, Australia*
V. Haverd, *CSIRO, Australia*
F. Hofhansl, *International Institute for Applied Systems Analysis, Austria*
J. Holm, *Lawrence Berkeley National Laboratory, United States*
B. Kruijt, *Alterra Wageningen, The Netherlands*
F. Leung, *Exeter University, United Kingdom*
B. E. Medlyn, *Western Sydney University, Australia*
L. M. Mercado, *Exeter University, United Kingdom*
R. J. Norby, *Oak Ridge National Laboratory, United States*
B. Pak, *CSIRO, Australia*
C.A. Quesada, *National Institute of Amazonian Research, Brazil*
C. von Randow, *National Institute for Space Research, Brazil*
K. J. Schaap, *National Institute of Amazonian Research, Brazil*
O. J. Valverde-Barrantes, *Florida International University, United States*
Y-P. Wang, *CSIRO, Australia*
X. Yang, *Oak Ridge National Laboratory, United States*
S. Zaehle, *Max-Planck Institute for Biogeochemistry, Germany*
Q. Zhu, *Lawrence Berkeley National Laboratory, United States*
D. M. Lapola, *University of Campinas, Brazil*
*corresponding author

Global terrestrial models currently predict that the Amazon rainforest will continue to act as a carbon sink in the future primarily due to the rising atmospheric carbon dioxide (CO_2) concentration, effectively enhancing its resilience and slowing the pace of climate change. Soil phosphorus impoverishment in parts of the Amazon basin limits biomass growth, but the role of phosphorus availability in limiting its future carbon uptake has not been considered in global model ensembles, e.g., during the 5th Climate Model Intercomparison Project (CMIP5). Here, we simulate a planned free-air CO_2 enrichment experiment in the Amazon with an ensemble of 14 terrestrial ecosystem models. The model ensemble represents diverse plant functional strategies and generates a series of testable hypotheses. We show that phosphorus availability reduces the projected CO_2-induced biomass carbon growth by about 50% to 79 ± 63 g C m^{-2} yr^{-1} over 15 years compared to estimates from carbon and carbon-nitrogen models. Our results suggest that the region's resilience to climate change may be much less than previously assumed. Variation in the biomass carbon response among the phosphorus-enabled models is considerable, ranging from 5 to 140 g C m^{-2} yr^{-1}, due to contrasting assumptions relating to the flexibility in plant phosphorus use and acquisition strategies. Experimental design needs to be targeted to reduce the uncertainties around the phosphorus feedback on the CO_2 fertilization effect.

The intact Amazon rainforest acts as a substantial carbon (C) sink, completely offsetting carbon dioxide (CO_2) emissions from fossil fuel combustion and land use change in the Amazon region[1,2]. Increasing atmospheric CO_2 concentrations from anthropogenic activity may be the primary factor for the current Amazon net C sink[1,3], via so-called CO_2 fertilization (an increase in photosynthetic C uptake by plants under higher CO_2), which is projected to continue into the future by global models[4–6]. The CO_2 fertilization effect has been observed experimentally in field experiments that were conducted predominantly in the temperate zone. In these experiments, the eCO_2 induced increase in C uptake was generally low when other factors, such as soil nitrogen (N), were limiting[7–9]. To date, whole-ecosystem-scale experiments, i.e., free-air CO_2 enrichment (FACE) have never been conducted in the tropics[10,11].

Over large parts of the Amazon and the tropics worldwide, phosphorus (P), not N, is assumed to be the key limiting nutrient, as most P has been lost or occluded from plant uptake during millions of years of soil pedogenesis[12,13]. Forests growing on these highly weathered old soils may nonetheless be highly productive due to the evolution of multiple strategies for P acquisition and use, enabling tight cycling of P between plants and soils[14,15]. Despite this

knowledge, quantifying the control of P on plant physiology, growth, and plant-soil interactions in global models, and hence its role in the forests' response to eCO_2, remains challenging[16,17]. This challenge is exacerbated by the scarcity of observations and distinctive species responses in hyperdiverse tropical forests[18].

Here, we study the potential interactions between eCO_2 and nutrient (N and P) feedbacks in a mature Amazonian rainforest by simulating the planned AmazonFACE experiment (+200 ppm; http://amazon-face.org/) with an ensemble of ecosystem models (n = 14, Extended Data Table 3), including three C, five carbon-nitrogen (CN), and six carbon-nitrogen-phosphorus (CNP) models[19–24]. The AmazonFACE experiment is located in a well-studied, highly productive tropical forest in Central Amazonia[25,26], growing on a strongly weathered *terra firme* Ferralsol. This ecosystem represents the low end of the plant-available P spectrum in the Amazon, consistent with ~32% of the Amazon rainforest's cover fraction[27]. *In situ* measurements were used to parameterise the models and to evaluate simulated ambient conditions (Extended Data Table 1, 2). Our aim was to generate *a priori* model-based hypotheses to highlight the state-of-the-knowledge and guide measurement strategies for AmazonFACE and other ecosystem manipulation experiments to gain crucial process understanding of P control on the CO_2 fertilization effect.

Simulated eCO_2 (+200 ppm) had a positive effect on plant biomass C across all models but was weakest in the CNP models (Fig. 1a). The eCO_2 conditions induced average biomass C gains of 163 ± 65, 145 ± 83, and 79 ± 63 g C m^{-2} yr^{-1} (mean ± SD) over 15 years in the C, CN and CNP models, respectively (Fig. 1a). Limitations by P thus reduced the predicted biomass C sink by 52% and 46% compared to that in the C and CN models, respectively, with considerable variation across and within model groups (Extended Data Fig. 1). Plot inventories at the AmazonFACE site during the 2000s indicate an aboveground biomass increment of 23 g C m^2 yr^{-1}, substantially below the Amazon-wide[1] estimate of 64 g C m^2 yr^{-1}. The model ensemble represents ambient conditions, such as productivity and leaf area index, reasonably well, but ensemble members show divergence in other ecosystem characteristics, such as the biomass C increment, which range from 5 to 114 g C m^2 yr^{-1}. There is, however, no clear pattern in performance between the model groups, so that we judge that these differences do not have bearing on the conclusions of our study (see more discussion in Extended Data Fig. 2).

Gross and net primary productivity (GPP and NPP, respectively) are both stimulated by eCO_2 in all models, both initially (after 1 year of eCO_2) and until the end of the simulation. The CNP models show the strongest decline from the initial response due to P limitation (Fig. 1b, c). The

final response of NPP to eCO_2 was a 35%, 29%, and 9% stimulation for the C, CN and CNP models, respectively. In general, in the CN and CNP models, nutrient limitation is defined as nutrient demand being greater than nutrient supply. However, models differ in their assumptions on how nutrient limitation controls productivity and C allocation in response to eCO_2, so that divergent responses on plant carbon use efficiency (CUE = NPP / GPP) are simulated (Extended Data Table 3). In some CN models, CUE increases because N limitation is hypothesized to reduce autotrophic respiration (Ra) via lower tissue N content. Some CNP models, however, assume a direct downregulation of growth and hence the plant CUE decreases (Extended Data Fig. 3). Elevated CO_2 induced higher fine root investments of NPP in some CN and CNP models to aid nutrient acquisition (Fig. 1c; Extended Data Fig. 4). Predicted changes in allocation with eCO_2 cause a general increase in biomass turnover across all but one of the models, partially offsetting the positive biomass response (Extended Data Table 4). Changes in turnover play a minor role in our 15 years simulation period but rather control the long-term future CO_2 effect on the biomass C sink[28,29].

Plant growth under eCO_2 is lowest in CNP models as the low availability of soil labile P restricts P uptake either immediately or over time (Extended Data Fig. 5). We considered the modelled P limitation on plant growth to be realistic, as the models and observations agree on soil labile P being very low (Extended Data Fig. 2). Other site observations support the fact that P is extremely critical for plant productivity, such as high leaf N:P ratios of 37 and high plant P resorption (before litter fall) of 78% (Extended Data Table 1). While P limitation consistently reduces the eCO_2-induced biomass C sink, there is significant variation among CNP models due to contrasting process representations (Fig. 2; Extended Data Table 3). P shortages downregulate growth (i.e., NPP) in all CNP models, directly or via photosynthesis. The major differences in the model assumptions relate to how they modify P supply and demand to alleviate plant P shortages, including either (i) enhancing plant P use efficiency (PUE = NPP / P uptake) or (ii) upregulating P acquisition mechanisms. The models assume that PUE may change if tissue nutrient ratios are flexible, if C allocation changes among tissues with different stoichiometry, and/or if P resorption is variable (Fig. 2). Flexible stoichiometry is considered in all CNP models except ELM-CTC, although with varying degrees of flexibility. Greater fine root C allocation with plant P stress is considered in some, and P resorption is a fixed fraction of leaf tissue P in all models (Fig. 2).

Models differ in their representation of soil P acquisition mechanisms; three of the six models (ELM-ECA, ELM-CTC, GDAY) consider desorption of P from mineral surfaces (i.e., the

secondary or strongly sorbed P pool), whereas the others assume P in those pools to be unavailable to plants. All the models include biochemical mineralization of organic P via phosphatase, but only three (ELM-ECA, ELM-CTC and ORCHIDEE) include the functionality to increase P acquisition via this mechanism under plant P stress (Fig. 2; Extended Data Table 3). Litter and soil stoichiometry are considered with varying degrees of flexibility. Soil labile P limits microbial decomposition rates of litter and soil, so that decomposition is reduced when immobilization demands for P exceed soil labile P availability (Fig. 2; Extended Data Table 3).

Diverging representations of plant P use and acquisition among the CNP models cause predictions of the eCO_2-induced biomass C sink to range from 5 g C m^{-2} yr^{-1} to 140 g C m^{-2} yr^{-1} (Fig. 3a; Extended Data Fig. 1). Greater plant PUE occurred in four of the models, for which shifts in tissue C:N and N:P due to eCO_2 led to increases in biomass C:P ranging from ~200 to 1600 g C g P^{-1} (Fig. 3c). Higher fine root investment with eCO_2, at the expense of less "P-costly" wood, offset some increases in PUE in some models. Flexible biomass stoichiometry altered decomposition dynamics and induced progressive P limitation in response to eCO_2, i.e., litter stoichiometry shifted towards lower quality (less N and P in relation to C), reducing net P mineralization rates from microbial decomposition, causing P to become increasingly unavailable to plants and accumulating in soil organic matter (Fig. 3d, e). This plant-soil-microbial feedback slowed the cycling of P in the ecosystem and exacerbated the initial P limitation (see Ref. [30] for a similar feedback during pedogenesis).

Enhanced plant P acquisition under eCO_2 effectively alleviated P limitation in two CNP models (ELM-CTC and ELM-ECA) (Fig. 3e). In both, eCO_2 increased the liberation of P from the secondary pool, as higher plant P demand and uptake diminished the labile P pool, in turn causing higher desorption rates. P desorption is thus only indirectly, and not mechanistically, enhanced by plants in these models. Biochemical mineralization of P under eCO_2 responded positively in both of the models, but added only notably to additional P acquisition in ELM-CTC (Fig. 3e). Although three CNP models simulated higher fine root investments, the actual P uptake return per fine root increment was marginal or came only into effect in the long-term (Extended Data Fig. 6).

Observations document ample N cycling in the system, e.g., high leaf N contents, indicative $\delta^{15}N$ values, high rates of N oxide emissions, and low leaf N resorption[31,32], and thereby suggest that plant growth is not directly affected by N availability. The CN models, however, simulate increased nitrogen use efficiency (NUE) and biomass C:N ratios, in response to insufficient N uptake under eCO_2 (Extended Data Fig. 5). Plant N availability may be underestimated in the

models, since the plant-available mineral N supply was <7 g N m^{-2} across all models, as opposed to 17.5 g N m^{-2} observed in the top 10 cm only (Extended Data Fig. 2). These results highlight an important gap in our knowledge also related to the dynamics of N availability, and its potential interaction with P dynamics (Table 1).

In summary, the model ensemble encapsulates a range of plausible hypotheses and represents a potential range of biomass C responses to eCO_2 under low soil P availability. The assumption of a lacking ability of plants to acquire more soil P and a limited capacity for plants to use P more efficiently resulted in effectively zero biomass C gain with eCO_2. Conversely, flexible stoichiometry, in combination with enhanced plant P acquisition, were the key mechanistic responses leading to biomass gain with eCO_2. Divergences in the simulated eCO_2 response lead us to the following testable hypotheses, and call for directed field measurements (Table 1):

H1. Low soil P availability will strongly constrain future plant biomass growth response to eCO_2 either by downregulating photosynthesis or limiting plant growth directly, or a combination thereof.

H2. Despite the limited soil P supply, plasticity in vegetation stoichiometry and allocation patterns will allow for some biomass growth under eCO_2.

H3. Plants will increase investments in P acquisition to increase P supply and allow biomass growth under eCO_2 either via greater P interception through fine root production or via greater P liberation from P desorption or biochemical mineralization of P.

These model-based hypotheses deepen a previous analysis of potential N and P limitation on C accumulation based on mass balance principle[33]. Furthermore, we add to a model intercomparison carried out in advance of the EucFACE experiment[34] by extending the range of plant P feedbacks considered across CNP models. This work highlighted H1: two stoichiometrically constrained CNP models predicted that strong P limitation will curtail the growth response to eCO_2 in Australia. Consistent with this hypothesis, aboveground growth has not increased with eCO_2 in that experiment over the initial years[35]. This finding underlines that monitoring efforts need to place a strong(er) focus on belowground carbon and nutrient dynamics, in addition to canopy-scale photosynthesis and aboveground growth dynamics. Additionally, Ra dependence on P content and plant stress from drought or nutrient limitation need further monitoring during experiments to fully elucidate the plant C budget and address H1 (Table 1).

Nutrient fertilization experiments support H2, as plasticity in leaf stoichiometry at the individual level, along with plasticity in P resorption efficiency, was observed[36]. Across the Amazon, community-weighted leaf N:P in the field varied from 13 to 42 g N g P^{-1} (n = 64) (Ref. [32]), which place our site, with a mean of 37, closer to the high end. GDAY predicted the most plausible increase in the leaf N:P ratio from 34 to 38 (Extended Data Fig. 7). Two models predicted strong increases in the leaf N:P ratio with eCO_2 but started off with much lower initial values. The degree to which plasticity in stoichiometry and resorption can aid plant PUE under eCO_2 in highly P-limited sites that are already at the end of the observed spectrum remains to be seen (H2). Monitoring plant tissue stoichiometry, including wood with much higher N:P ratios, combined with assessments of P resorption in CO_2 and nutrient fertilization experiments will reduce uncertainties (Table 1).

Based on previous observations[8], a number of models assume increased fine root investment, as well as higher biochemical P mineralization and P desorption from mineral surfaces, under eCO_2-induced nutrient limitation (H3). The effect of increased fine root biomass on nutrient uptake was limited in our simulations and ambient fine root allocation fractions were highly variable among the models, ranging from 5-30% of NPP (Extended Data Fig. 4, 6). Both these modelled results highlight model deficiencies in belowground processes[37] that need addressing (Table 1). There is evidence that phosphatase activity in litter and soil and the presence of low-molecular-weight acids used to liberate P from organic matter or from mineral surfaces increase with plant P demand[38]. This was predicted by ELM-CTC in our simulations, which also showed Amazon-wide that "[with] enhanced phosphatase production, productivity in the highly P-limited areas can be sustained under elevated CO_2 conditions"[39]. Plants invest in P liberation and acquisition, but if these mechanisms can be upregulated under eCO_2 and over what time frame this may occur remain open questions. Quantification of such a response is lacking, as are estimates of the associated plant C costs to acquire P via these and other mechanisms, such as mycorrhizal symbiosis[15,40] (Table 1). The P gain and C cost for P acquisition mechanisms, as well as the associated plant-soil-microbial interactions, need to be assessed by analyses of soil, microbial and root nutrition, and via novel techniques investigating enzyme and labile C dynamics[41]. Monitoring of belowground fine root dynamics needs to include the surface litter layer, commonly explored by fine roots in P-impoverished ecosystems in the Amazon, not yet quantified nor considered in models (Table 1).

Previous model projections suggest a sustained fertilization effect of CO_2 on the Amazon C sink but have not considered feedbacks from low soil P availability[5,6]. Our study demonstrates

that, based on the current generation of CNP models, the omission of P feedbacks is highly likely to cause an overestimation of the Amazon rainforest's capacity to sequester atmospheric CO_2. Considering P limitation on the CO_2 fertilization effect in future predictions may indicate that the forest is less resilient to higher temperatures and changing rainfall patterns than previously thought[6,42]. Periods of water deficit may contribute to the eCO_2 fertilization effect on productivity due to its water saving effect[34], or due to alterations of decomposition processes. Our study site experienced years with significantly less than average precipitation, e.g. in 2000 and 2009, however, in our simulations this increased the positive response of GPP and NPP to eCO_2 only marginally (Extended Data Figure 8 and 9). Models lack the appropriate sensitivity of plant responses to changes in water availability, and even more so when precipitation sums are that high[43]. Interactions of water and P availability and their consequences on the CO_2 fertilization effect remain uncertain[44] and is an area where field measurements will allow us to better constrain model responses (Table 1).

Although P is likely to reduce the biomass C sink response to CO_2 in regions with low plant-available P supply, our results suggest that plasticity in plant P use and plant P acquisition mechanisms, may at least partially alleviate P limitation under eCO_2 and enable CO_2 fertilization of biomass growth. The model ensemble may be interpreted as representing a range of possible tropical plant functional strategies and growth responses to low P availability under eCO_2. Responses are expected to be species-specific, as were plant growth responses to low P supplies in another tropical region[18]. The ecosystem-scale response to P limitation under eCO_2 will thus depend on the relative contributions of the various P acquisition and P use strategies across individuals, their interactions and to what extent these processes can be upregulated under eCO_2. All of which ultimately need to be described and represented in a single model framework in order to accurately predict the Amazon rainforest's response to future climate change.

AmazonFACE has the unique opportunity to experimentally address these key areas of uncertainty, not only by integrating the proposed measurements across seasons and at the ecosystem scale (summary in Table 1) but also by assessing species-specific responses to eCO_2 in relation to trait expression. Amazon-wide expression of plant functional strategies may then be inferred by applying the mechanistic interplay between trait expression and edaphic conditions. The key to predicting the future of the world's largest tropical forest under eCO_2 thus lies in obtaining experimental data on, and subsequently modelling, different plant P acquisition and use strategies, as well as their interactions in a competing plant community.

END NOTES

Author contributions

D.M.L., A.R., and K.F. conceived the study. L.F., S.G., A.G., F.H., R.N., C.A.Q., K.J.S., and O.J.V.-B. collected field data. K.F., D.G., M. de K., M.J., V.H., J.H., F.L., L.M.M., B.P., C.v.R., Y.-P.W., X.Y., S.Z., and Q.Z. performed model simulations. K.F. wrote the manuscript with contributions from all co-authors.

Acknowledgements

We thank the many scientists involved in the development of the models used in our study; the many scientists, field and laboratory technicians and other staff involved in collecting and analysing the field data; and everyone involved in the planning and conductance of the AmazonFACE project. Oak Ridge National Laboratory is operated by UT-Battelle, LLC, under contract DE-AC05-00OR22725 with the US Department of Energy. We thank the DFG for financing the workshop that made this study possible (grant No. RA 2060/4-1) and for providing funds to K.F. (grant No. RA 2060/5-1.)

REFERENCES

1. Brienen, R. J. W. *et al.* Long-term decline of the Amazon carbon sink. *Nature* **519,** 344–348 (2015).

2. Phillips, O. L. & Brienen, R. J. W. Carbon uptake by mature Amazon forests has mitigated Amazon nations' carbon emissions. *Carbon Balance Manag.* **12,** 1 (2017).

3. Cernusak, L. A. *et al.* Tropical forest responses to increasing atmospheric CO2: Current knowledge and opportunities for future research. *Funct. Plant Biol.* **40,** 531–551 (2013).

4. Ciais, P. *et al.* The physical science basis. Contribution of working group I to the fifth assessment report of the intergovernmental panel on climate change. *Chang. IPCC Clim.* 465–570 (2013).

5. Cox, P. M. *et al.* Sensitivity of tropical carbon to climate change constrained by carbon dioxide variability. *Nature* **494,** 341–344 (2013).

6. Huntingford, C. *et al.* Simulated resilience of tropical rainforests to CO$_2$-induced climate change. *Nat. Geosci.* **6,** 268–273 (2013).

7. Talhelm, A. F. *et al.* Elevated carbon dioxide and ozone alter productivity and

294 ecosystem carbon content in northern temperate forests. *Glob. Chang. Biol.* **20,** 2492–
295 2504 (2014).

296 8. Norby, R. J., Warren, J. M., Iversen, C. M., Medlyn, B. E. & McMurtrie, R. E. CO2
297 enhancement of forest productivity constrained by limited nitrogen availability. *Proc.*
298 *Natl. Acad. Sci.* **107,** 19368–19373 (2010).

299 9. Zaehle, S. *et al.* Evaluation of 11 terrestrial carbon-nitrogen cycle models against
300 observations from two temperate Free-Air CO2Enrichment studies. *New Phytol.* **202,**
301 803–822 (2014).

302 10. Hofhansl, F. *et al.* Amazon forest ecosystem responses to elevated atmospheric CO2
303 and alterations in nutrient availability: filling the gaps with model-experiment
304 integration. *Front. Earth Sci.* **4,** (2016).

305 11. Norby, R. J. *et al.* Model-data synthesis for the next generation of forest free-air CO2
306 enrichment (FACE) experiments. *New Phytol.* **209,** 17–28 (2016).

307 12. Lloyd, J., Bird, M. I., Veenendaal, E. M. & Kruijt, B. Should Phosphorus Availability
308 Be Constraining Moist Tropical Forest Responses to Increasing CO2 Concentrations?
309 *Glob. Biogeochem. Cycles Clim. Syst.* 95–114 (2001).

310 13. Vitousek, P. M. Litterfall, nutrient cycling, and nutrient limitation in tropical forests.
311 *Ecology* **65,** 285–298 (1984).

312 14. Quesada, C. A. *et al.* Basin-wide variations in Amazon forest structure and function are
313 mediated by both soils and climate. *Biogeosciences* **9,** 2203–2246 (2012).

314 15. Lambers, H., Raven, J. A., Shaver, G. R. & Smith, S. E. Plant nutrient-acquisition
315 strategies change with soil age. *Trends Ecol. Evol.* **23,** 95–103 (2008).

316 16. Reed, S. C., Yang, X. & Thornton, P. E. Incorporating phosphorus cycling into global
317 modeling efforts: A worthwhile, tractable endeavor. *New Phytol.* **208,** 324–329 (2015).

318 17. Jiang, M., Caldararu, S., Zaehle, S., Ellsworth, D. S. & Medlyn, B. E. Towards a more
319 physiological representation of vegetation phosphorus processes in land surface
320 models. *New Phytol.* 1–7 (2019).

321 18. Turner, B. L., Brenes-Arguedas, T. & Condit, R. Pervasive phosphorus limitation of
322 tree species but not communities in tropical forests. *Nature* **555,** 367–370 (2018).

323 19. Goll, D. S. *et al.* A representation of the phosphorus cycle for ORCHIDEE (revision

4520). *Geosci. Model Dev.* **10,** 3745–3770 (2017).

20. Wang, Y.-P., Law, R. M. & Pak, B. A global model of carbon, nitrogen and phosphorus cycles for the terrestrial biosphere. *Biogeosciences* **7,** 2261–2282 (2010).

21. Haverd, V. *et al.* A new version of the CABLE land surface model (Subversion revision r4601) incorporating land use and land cover change, woody vegetation demography, and a novel optimisation-based approach to plant coordination of photosynthesis. *Geosci. Model Dev.* **11,** 2995–3026 (2018).

22. Comins, H. N. & McMurtrie, R. E. Long-Term Response of Nutrient-Limited Forests to CO"2 Enrichment; Equilibrium Behavior of Plant-Soil Models. *Ecol. Appl.* **3,** 666–681 (1993).

23. Zhu, Q., Riley, W. J., Tang, J. & Koven, C. D. Multiple soil nutrient competition between plants, microbes, and mineral surfaces: model development, parameterization, and example applications in several tropical forests. *Biogeosciences* **13,** 341–363 (2016).

24. Yang, X., Thornton, P. E., Ricciuto, D. M. & Post, W. M. The role of phosphorus dynamics in tropical forests – a modeling study using CLM-CNP. *Biogeosciences* **11,** 1667–1681 (2014).

25. Malhi, Y. *et al.* Comprehensive assessment of carbon productivity, allocation and storage in three Amazonian forests. *Glob. Chang. Biol.* **15,** 1255–1274 (2009).

26. Araújo, A. C. *et al.* Comparative measurements of carbon dioxide fluxes from two nearby towers in a central Amazonian rainforest: The Manaus LBA site. *J. Geophys. Res.* **107,** 8090 (2002).

27. Quesada, C. A. *et al.* Soils of Amazonia with particular reference to the RAINFOR sites. *Biogeosciences* **8,** 1415–1440 (2011).

28. Friend, A. D. *et al.* Carbon residence time dominates uncertainty in terrestrial vegetation responses to future climate and atmospheric CO $_2$. *Proc. Natl. Acad. Sci.* **111,** 3280–3285 (2014).

29. Walker, A. P. *et al.* Predicting long-term carbon sequestration in response to CO2 enrichment: How and why do current ecosystem models differ? *Global Biogeochem. Cycles* **29,** 476–495 (2015).

30. Vitousek, P. M. *Nutrient cycling and limitation: Hawai'i as a model system*. *Princeton*

University Press (2004).

31. Nardoto, G. B. *et al.* Basin-wide variations in Amazon forest nitrogen-cycling characteristics as inferred from plant and soil 15N:14N measurements. *Plant Ecol. Divers.* **7,** 173–187 (2014).

32. Fyllas, N. M. *et al.* Basin-wide variations in foliar properties of Amazonian forest: phylogeny, soils and climate. *Biogeosciences* **6,** 2677–2708 (2009).

33. Wieder, W. R., Cleveland, C. C., Smith, W. K. & Todd-Brown, K. Future productivity and carbon storage limited by terrestrial nutrient availability. *Nat. Geosci.* **8,** 441–444 (2015).

34. Medlyn, B. E. *et al.* Using models to guide field experiments: a priori predictions for the CO2 response of a nutrient- and water-limited native Eucalypt woodland. *Glob. Chang. Biol.* **22,** 2834–2851 (2016).

35. Ellsworth, D. S. *et al.* Elevated CO2 does not increase eucalypt forest productivity on a low-phosphorus soil. *Nat. Clim. Chang.* **7,** 279–282 (2017).

36. Wright, S. J. *et al.* Plant responses to fertilization experiments in lowland, species-rich, tropical forests. *Ecology* **99,** 1129–1138 (2018).

37. Warren, J. M. *et al.* Root structural and functional dynamics in terrestrial biosphere models--evaluation and recommendations. *New Phytol.* **205,** 59–78 (2015).

38. Hoosbeek, M. R. Elevated CO2 increased phosphorous loss from decomposing litter and soil organic matter at two FACE experiments with trees. *Biogeochemistry* **127,** 89–97 (2016).

39. Yang, X., Thornton, P. E., Ricciuto, D. M. & Hoffman, F. M. Phosphorus feedbacks constraining tropical ecosystem responses to changes in atmospheric CO2 and climate. *Geophys. Res. Lett. Res.* 7205–7214 (2016).

40. Vicca, S. *et al.* Fertile forests produce biomass more efficiently. *Ecol. Lett.* **15,** 520–526 (2012).

41. Wang, Y. & Lambers, H. Root-released organic anions in response to low phosphorus availability: recent progress, challenges and future perspectives. *Plant Soil* (2019).

42. Gatti, L. V. *et al.* Drought sensitivity of Amazonian carbon balance revealed by atmospheric measurements. *Nature* **506,** (2014).

43. Powell, T. L. *et al.* Confronting model predictions of carbon fluxes with measurements of Amazon forests subjected to experimental drought. *New Phytol.* **200,** 350–365 (2013).

44. He, M. & Dijkstra, F. A. Drought effect on plant nitrogen and phosphorus: A meta-analysis. *New Phytol.* **204,** 924–931 (2014).

392 Table 1. List of key processes and variables that need to be constrained by observational
393 estimates in order reduce uncertainty in P cycle control on the eCO_2 effect ecosystem models.

(H1) Plant C budget	**Measurements needed**
Canopy scale C assimilation	• Seasonal dynamics of leaf area and photosynthetic capacity • Photosynthetic acclimation
Plant tissue respiration	• Control of drought stress, nutrient limitation and P content • Wood and root respiration
Biomass growth	• Belowground biomass compartments • Long term growth rates
(H2) Plant P use	
Plant tissue C:P and N:P stoichiometry	• Plasticity versus adaptability to (experimental) change in eCO_2 or nutrient availability • Functionality of tissue P • Wood P content /stoichiometry
Plant tissue P resorption	• P content in live tissue and fresh litter • Plasticity versus adaptability to (experimental) change in eCO_2 or nutrient availability
(H3) Plant P acquisition	
P desorption due to plant exudation	• Interactions with microorganisms (directly or via microorganisms) • Cost of exudation vs. plant P uptake
P acquisition due to fine root production	• Surface litter activity • Fine root allocation fractions • Fine root productivity vs. plant P uptake
Biochemical P mineralization (via phosphatase)	• Phosphatase activity and relation to P mineralization • Plant production of phosphatase vs. plant-induced production by microorganisms • Cost of phosphatase production vs. plant P acquisition
Other interactions	
Plant N availability	• Ecosystem N budget • Symbiotic and free-living N fixation • Control of N availability on P acquisition
Plant water availability	• Control on P mineralization and transport dynamics • Control on of water and P limitation on eCO_2 effect

394

METHODS

Site description

Model simulations were conducted at the AmazonFACE experimental site in Central Amazonia (2º35'39" S, 60º12'29'' W). AmazonFACE is an integrated model-experiment project that aims to assess the effects of high CO_2 concentrations on the ecology and resilience of the Amazon rainforest (http://amazon-face.org/). The experiment is currently being established and is situated in a *terra firme* forest on a plateau characterized by highly weathered, deep, clay sediment soil (with a clay fraction of 76%), classified as a Geric Ferrasol[1]. The site and the surrounding area have been subjected to various long-term measurement activities[2–6], coordinated by the Large-Scale Biosphere-Atmosphere Program (LBA; http://lba2.inpa.gov.br/) in Amazonia, including the "K34" eddy covariance flux tower[7], located approximately 2 km away from AmazonFACE site. Mean annual precipitation at K34 from January 2000 to December 2015 was 2600 mm yr^{-1}, and the mean temperature was 26°C.

Model descriptions

Fourteen ecosystem models with contrasting representations of ecosystem functioning and nutrient cycling were applied to the experiment (Extended Data Table 3). C cycle dynamics without nutrient cycle feedbacks are represented in the "C-only" models (InLand, ED2 and ELM-FATES)[8–10]; C and N dynamics are represented in the "CN" models (LPJ-GUESS, O-CN, JULES, CABLE-POP(CN) and GDAY(CN))[11–13]; and C, N, and P dynamics are represented in the "CNP" models (ELM-ECA, ELM-CTC, CABLE, CABLE-POP, ORCHIDEE, and GDAY)[14–19]. Four of the models are dynamic vegetation models: CABLE-POP considers dynamic establishment and mortality with fixed plant functional type (PFT) composition, while LPJ-GUESS, ED2 and ELM-FATES also consider dynamic PFT composition. Photosynthesis is based on formulations by Farquahar[20] or derivations thereof in all of the models[21,22] (Extended Data Table 3).

Prognostic C allocation fractions are based on functional relationships among tissues, e.g., fixed ratios between sapwood and leaf area in CABLE-POP, LPJ-GUESS, ED2, GDAY, ORCHIDEE, O-CN, JULES, and ELM-FATES, and on resource dependence, e.g., higher root allocation under water or nutrient stress in LPJ-GUESS, ELM-ECA, GDAY, O-CN, ORCHIDEE, ED2 and ELM-FATES. C allocation fractions are fixed in InLand and CABLE.

Nutrient limitation is determined by the difference between demand and supply (via root uptake and resorption) of N or P, with the most limiting nutrient determining the degree of limitation. The photosynthetic parameters V_{cmax} and/or J_{max} are controlled by leaf N in all CN and CNP models except JULES, while leaf P additionally downregulates gross primary productivity (GPP) in all CNP models except ORCHIDEE. N controls net primary productivity (NPP) in some of the models, i.e., O-CN, JULES, ORCHIDEE, CABLE and CABLE-POP, and additionally downregulates growth efficiency (GPP/LAI) in CABLE and CABLE-POP.

Maintenance respiration is dependent on temperature in all models and is additionally controlled by tissue N content in all of the models that consider the N cycle with the exception of GDAY, where Ra is a fixed fraction of GPP. Plant tissue stoichiometry in the CN and CNP models is either fixed (ELM-CTC and JULES) or varies within or without bounds (all other models). The nutrient resorption rates in the CN and CNP models are always fixed fractions of the nutrient content in leaves and roots. Competition for nutrients between plant uptake and decomposition processes is handled differently. Nutritional demands for the decomposition process (representing microbial demands) are met entirely first in some models (CABLE, O-CN, ORCHIDEE, and GDAY), are based on relative demands between decomposition and plant uptake (ELM-CTC), or are determined via a multiple consumer approach including adsorption to mineral surfaces (ELM-ECA). Nutrient uptake is a function of plant demand and nutrient availability in all models and is further controlled by a measure of root mass in LPJ-GUESS, GDAY, ORCHIDEE, and O-CN.

Soil organic matter (SOM) decomposition is limited by soil mineral N availability in most CN and CNP models (except O-CN and ORCHIDEE) and additionally by labile P availability in most CNP models (except GDAY and ORCHIDEE). P in SOM can also be mineralized via phosphatase, decoupling the P cycle from the C and N cycle, termed biochemical P mineralization in the P models. Biochemical P mineralization is a function of the slow SOM pool turnover in CABLE, CABLE-POP and GDAY, as well as substrate availability in ORCHIDEE, ELM-ECA and ELM-CTC. Biochemical P mineralization is upregulated with higher plant P stress, representing higher phosphate production (not specified if by plants or microbes), in ELM-ECA, ELM-CTC and ORCHIDEE.

N inputs originate from N deposition (prescribed by model protocol) and N fixation (prescribed individually). N fixation is either fixed, calculated empirically as a fraction of NPP or

evapotranspiration (GDAY, JULES, ORCHIDEE, ALM-CTC, LPJ-GUESS, CABLE, and CABLE-POP), or based on an optimization scheme (ELM-ECA and O-CN). P inputs originate from weathering (prescribed individually) and deposition (prescribed by model protocol). Release of P from rock weathering is a fixed, soil type-specific rate in CABLE and CABLE-POP, a function of the parent P pool in ELM-ECA, ELM-CTC, and GDAY or described as a function of lithology, runoff and air temperature in ORCHIDEE. N and P losses occur from leaching, modelled as a function of the size of the labile P and mineral N pool, respectively, and additionally controlled by runoff in ELM-ECA and ORCHIDEE.

The number of inorganic P pools and their precise definition varies among the models. We consider two inorganic P pools relevant for our analysis: the labile P pool and the secondary P pool. The labile P pool encompasses plant-available inorganic P, represented in most CNP models by two separate pools connected by sorption dynamics and effectively in equilibrium (described by Langmuir dynamics in most models and a linear approach in ORCHIDEE). The labile P pools follow different nomenclature in the models but are comparable in functionality: the P in soil solution (called labile or solution P) is readily available to plants in the model time step, while the non-dissolved P (referred to as sorbed or sorbed labile P pool) can become available to plants on yearly to decadal time scales due to desorption. The secondary P pool represents P strongly sorbed by minerals, which is largely unavailable but may enter the labile P pool on centennial time scales and, depending on model assumptions, may be driven by plant P stress.

Model simulations

Models were forced with 16 years of observed local meteorology (2000 to 2015) from the K34 flux tower[7]. Meteorological data from July 1999 to December 2015 of near-surface air temperature, rainfall, downward shortwave radiation, downward longwave radiation, vapour pressure deficit, surface pressure, relative humidity, and wind speed were available for model input. Specific humidity was calculated based on observed relative humidity and surface pressure. All data time series were subject to quality control (i.e., removal of outliers) and gap filling using the variables' climatological mean. Precipitation data gaps were filled from a nearby weather station of the Tropical Rainfall Measuring Mission network.

Simulations are initialized with a spin-up routine resulting in equilibrium conditions of C stocks (and N, and P, if applicable) representing the year 1850. The 16-year meteorological time series

are continuously repeated throughout the whole spin-up, during the transient phase (1851 to 1998), and during our model-experiment phase (1999 to 2013), representative of a 15-year long AmazonFACE experiment. Global datasets are used as inputs for atmospheric CO_2[23,24], N deposition[25,26], and P deposition[27]. Atmospheric CO_2, N and P deposition levels were set to 284.7 ppm, 1.43 kg N ha^{-1} yr^{-1}, and 0.144 kg P ha^{-1} yr^{-1} in 1850, respectively, and follow historical changes during the transient and model experiment phase.

Other site parameters used for parameterization of the models are derived from *in situ* measurements and include rooting and soil depth (set to rooting depth), soil hydraulic parameters, specific leaf area (SLA), and soil texture (Extended Data Table 2). Soil hydraulic parameters are derived from pedotransfer functions[28] and site-specific measurements of soil properties[29]. Soil hydraulic parameters were included in models that accounted for this functionality to allow for a better representation of soil water dynamics in tropical soils (Extended Data Table 2).

Two model experiments are performed over the 15-year long experiment phase by each model to assess the effect of elevated CO_2: 1) the ambient run (AMB) and 2) the elevated CO_2 run (ELE). In the AMB run, the atmospheric CO_2 is set to ambient levels and is employed for model evaluation against *in situ* measurements, including C fluxes from the K34 flux tower. The ELE run represents the planned AmazonFACE experiment with a step change increase of 200 ppm at the start of the model experiment and continuous tracking of CO_2 levels in AMB plus 200 ppm thereafter. Model outputs are analysed in biological years of seasonality (July to June), and the difference between the elevated CO_2 run and the control run are used to infer the model-based CO_2 effect.

Model output analysis

The analysis of the modelled output includes the evaluation of modelled ambient conditions relative to *in situ* observations and hypotheses-based analyses of the modelled CO_2 responses. We employ a structural analysis of the model simulations[30–32], splitting model outcomes into the underlying processes to identify crucial model assumptions determining diverging predictions for the FACE experiment. We focus on the simulated increase in biomass C due to eCO_2 and the underlying nutrient control thereon.

Biomass C dynamics are a result of primary productivity, C allocation and turnover. We first analyse the effect of eCO_2 on gross primary productivity (GPP), net primary productivity (NPP), autotrophic respiration (Ra), and the resulting plant carbon use efficiency (CUE), where CUE =

NPP/GPP. We then assess changes in NPP allocation fractions to biomass compartments of wood, fine roots and leaves, and the resulting effect on biomass C turnover in response to eCO_2. Specific tissue turnover rates are fixed in all models, but overall biomass C turnover changes as a result of changing C allocation to tissue compartments. Turnover rates of biomass C pools are calculated as the fraction of total litter fall per total biomass pool size (Extended Data Table 4).

Plant nutrient cycle feedbacks to eCO_2 are assessed by splitting the responses into plant N uptake (NUP) and plant N use efficiency (NUE), where NUE = NPP/NUP, and similarly into P uptake (PUP) and P use efficiency (PUE), where PUE = NPP/PUP. The responses of NUE and PUE to eCO_2 are further split into changes in tissue C allocation (differing in C:N and N:P ratios) and changes in tissue stoichiometry (flexible C:N and N:P ratios). Soil nutrient cycle feedbacks to eCO_2 are determined by separating eCO_2 responses in N and P mineralization rates (N and P mineralization from microbial decomposition of SOM and biochemical P mineralization of organic P via phosphatase) and the balance of ecosystem N and P inputs (N fixation, N and P deposition, and P weathering) and losses (N and P leaching).

DATA AVAILABILITY STATEMENT

The model driving data and model outputs will be made publicly available on figshare under https://figshare.com/ once the manuscript is accepted. Site data used for model evaluation and calibration are available in the Supplementary Information. All other data are available from the corresponding author upon reasonable request.

REFERENCES METHODS

1. Quesada, C. A. *et al.* Variations in chemical and physical properties of Amazon forest soils in relation to their genesis. *Biogeosciences* **7,** 1515–1541 (2010).

2. Chambers, J. Q. *et al.* Respiration from a Tropical Forest Ecosystem : Partitioning of Sources and Low Carbon Use Efficiency. *Ecol. Appl.* **14,** 72–88 (2004).

3. Malhi, Y. *et al.* Comprehensive assessment of carbon productivity, allocation and storage in three Amazonian forests. *Glob. Chang. Biol.* **15,** 1255–1274 (2009).

4. Aragão, L. E. O. C. *et al.* Above- and below-ground net primary productivity across ten Amazonian forests on contrasting soils. *Biogeosciences* **6,** 2759–2778 (2009).

5. Holm, J. A., Chambers, J. Q., Collins, W. D. & Higuchi, N. Forest response to increased disturbance in the central Amazon and comparison to western Amazonian forests. *Biogeosciences* **11,** 5773–5794 (2014).

6. Hadlich, H. L. *et al.* Recognizing Amazonian tree species in the field using bark tissues spectra. *For. Ecol. Manage.* **427,** 296–304 (2018).

7. Araújo, A. C. *et al.* Comparative measurements of carbon dioxide fluxes from two nearby towers in a central Amazonian rainforest: The Manaus LBA site. *J. Geophys. Res.* **107,** 8090 (2002).

8. Kucharik, C. J. *et al.* Testing the performance of a dynamic global ecosystem model: Water balance, carbon balance, and vegetation structure. *Global Biogeochem. Cycles* **14,** 795–825 (2000).

9. Fisher, R. A. *et al.* Taking off the training wheels : the properties of a dynamic vegetation model without climate envelopes, CLM4.5 (ED). 3593–3619 (2015).

10. Medvigy, D., Wofsy, S. C., Munger, J. W., Hollinger, D. Y. & Moorcroft, P. R. Mechanistic scaling of ecosystem function and dynamics in space and time: Ecosystem Demography model version 2. *J. Geophys. Res. Biogeosciences* **114,** (2009).

11. Smith, B. *et al.* Implications of incorporating N cycling and N limitations on primary production in an individual-based dynamic vegetation model. *Biogeosciences* **11,** 2027–2054 (2014).

12. Zaehle, S. & Friend, A. D. Carbon and nitrogen cycle dynamics in the O-CN land surface model: 1. Model description, site-scale evaluation, and sensitivity to parameter estimates. *Global Biogeochem. Cycles* **24,** 1–13 (2010).

13. Best, M. J. *et al.* The Joint UK Land Environment Simulator (JULES), model description Part 1: Energy and water fluxes. *Geosci. Model Dev.* **4,** 677–699 (2011).

14. Zhu, Q., Riley, W. J., Tang, J. & Koven, C. D. Multiple soil nutrient competition between plants, microbes, and mineral surfaces: model development, parameterization, and example applications in several tropical forests. *Biogeosciences* **13,** 341–363 (2016).

15. Yang, X., Thornton, P. E., Ricciuto, D. M. & Post, W. M. The role of phosphorus dynamics in tropical forests - a modeling study using CLM-CNP. *Biogeosciences* **11,** 1667–1681 (2014).

16. Wang, Y. P., Law, R. M. & Pak, B. A global model of carbon, nitrogen and phosphorus cycles for the terrestrial biosphere. *Biogeosciences* **7,** 2261–2282 (2010).

17. Haverd, V. *et al.* A new version of the CABLE land surface model (Subversion revision r4601) incorporating land use and land cover change, woody vegetation demography, and a novel optimisation-based approach to plant coordination of photosynthesis. *Geosci. Model Dev.* **11,** 2995–3026 (2018).

18. Goll, D. S. *et al.* A representation of the phosphorus cycle for ORCHIDEE (revision 4520). *Geosci. Model Dev.* **10,** 3745–3770 (2017).

19. Comins, H. N. & McMurtrie, R. E. Long-Term Response of Nutrient-Limited Forests to CO"2 Enrichment; Equilibrium Behavior of Plant-Soil Models. *Ecol. Appl.* **3,** 666–681 (1993).

20. Farquhar, G. D., von Caemmerer, S. & Berry, J. A. A biochemical model of photosynthetic CO2 assimilation in leaves of C3 species. *Planta* **149,** 78–90 (1980).

21. Collatz, G. J., Ball, J. T., Grivet, C. & Berry, J. A. Physiological and Environmental-Regulation of Stomatal Conductance, Photosynthesis and Transpiration - a Model That Includes a Laminar Boundary-Layer. *Agric. For. Meteorol.* **54,** 107–136 (1991).

22. Kull, O. & Kruijt, B. Leaf photosynthetic light response: A mechanistic model for scaling photosynthesis to leaves and canopies. *Funct. Ecol.* **12,** 767–777 (1998).

23. Etheridge, D. M. *et al.* Natural and anthropogenic changes in atmospheric CO_2 over the last 1000 years from air in Antarctic ice and firn. *J. Geophys. Res. Atmos.* **101,** 4115–4128 (1996).

595 24. MacFarling Meure, C. *et al.* Law Dome CO_2, CH_4 and N_2O ice core records extended
596 to 2000 years BP. *Geophys. Res. Lett.* **33,** L14810 (2006).

597 25. Lamarque, J. F. *et al.* Historical (1850-2000) gridded anthropogenic and biomass burning
598 emissions of reactive gases and aerosols: Methodology and application. *Atmos. Chem.*
599 *Phys.* **10,** 7017–7039 (2010).

600 26. Lamarque, J. F. *et al.* Global and regional evolution of short-lived radiatively-active gases
601 and aerosols in the Representative Concentration Pathways. *Clim. Change* **109,** 191–212
602 (2011).

603 27. Wang, R. *et al.* Global forest carbon uptake due to nitrogen and phosphorus deposition
604 from 1850 to 2100. *Glob. Chang. Biol.* **23,** 4854–4872 (2017).

605 28. Tomasella, J. & Hodnett, M. Pedotransfer functions for tropical soils. in *Developments in*
606 *Soil Science* **30,** 415–429 (Elsevier, 2004).

607 29. Marthews, T. R. *et al.* High-resolution hydraulic parameter maps for surface soils in
608 tropical South America. *Geosci. Model Dev.* **7,** 711–723 (2014).

609 30. De Kauwe, M. G. *et al.* Where does the carbon go? A model-data intercomparison of
610 vegetation carbon allocation and turnover processes at two temperate forest free-air
611 CO2enrichment sites. *New Phytol.* **203,** 883–899 (2014).

612 31. Walker, A. P. *et al.* Comprehensive ecosystem model-data synthesis using multiple data
613 sets at two temperate forest free-air CO2 enrichment experiments: Model performance at
614 ambient CO2 concentration. *J. Geophys. Res. Biogeosciences* **119,** 937–964 (2014).

615 32. Zaehle, S. *et al.* Evaluation of 11 terrestrial carbon-nitrogen cycle models against
616 observations from two temperate Free-Air CO2 Enrichment studies. *New Phytol.* **202,**
617 803–822 (2014).

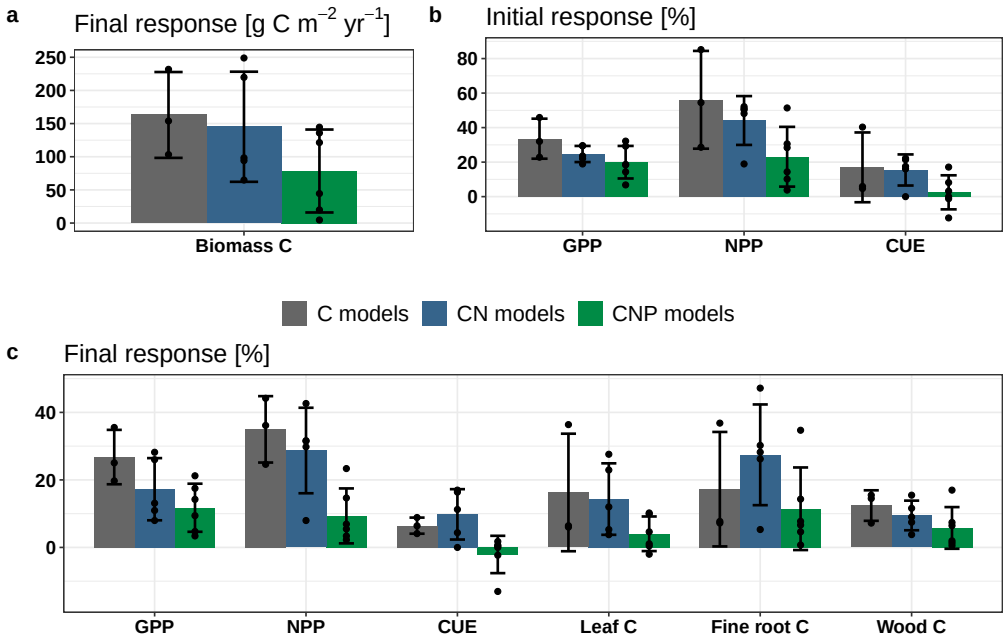

Figure 1: **The predicted effect of eCO_2 on biomass C, productivity and biomass compartments**, averaged over C (grey), CN (blue) and CNP (green) model groups. **a**, The final absolute response of biomass growth, calculated as the mean annual response over the 15 years of eCO_2 per model group in g C m^{-2} yr^{-1}. **b**, Initial relative responses of productivity (GPP and NPP), and CUE (=NPP/GPP) in %, calculated as the mean response in the first year. **c**, Final relative responses of productivity and CUE, as well as total leaf, fine root and wood C, calculated as the mean response after 15 years (mean of 13th to 17th year), all in %. Responses to eCO_2 are the differences between the elevated and ambient model run, shown as mean and standard deviation per model group, and individual model results as dots. See also corresponding Extended Data Figure 1 and 3.

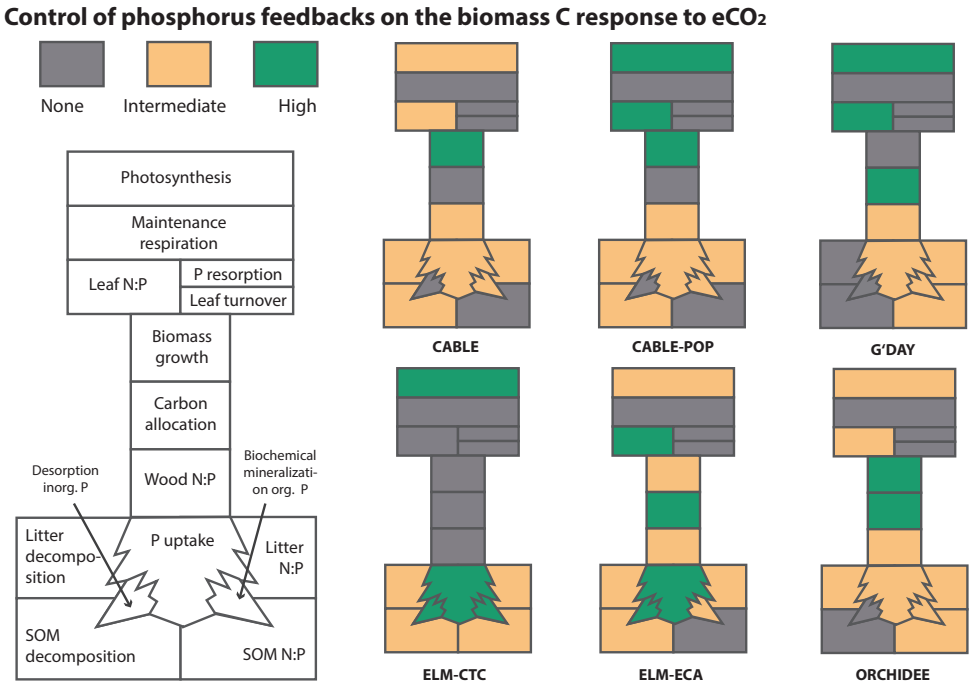

Figure 2: **Strength of phosphorus feedbacks in controlling the biomass C response to eCO_2 for the six CNP models.** Ecosystem processes are highlighted that depend (or not depend) on the P cycle, for which classes (none, intermediate, high) indicate the degree to which the considered P feedback causes a response of biomass C to eCO_2 in our simulations. P limitation causes strong or intermediate downregulation of photosynthesis with eCO_2 across all models. Maintenance respiration, leaf turnover and P resorption are not responsive to P feedbacks in any of the models. Leaf N:P responds to eCO_2 in most models, but is fixed in ELM-CTC, narrowly bound in CABLE, and at its maximum in ORCHIDEE. P limitation causes direct downregulation of biomass growth in CABLE, CABLE-POP, ELM-ECA and ORCHIDEE. Allocation shifts towards roots to alleviate P limitation is considered in GDAY, ELM-ECA and ORCHIDEE. Desorption of P from mineral surfaces is only considered in ELM-ECA and ELM-CTC, and biochemical P mineralization is considered in many models, but only effectively responsive in ELM-CTC.

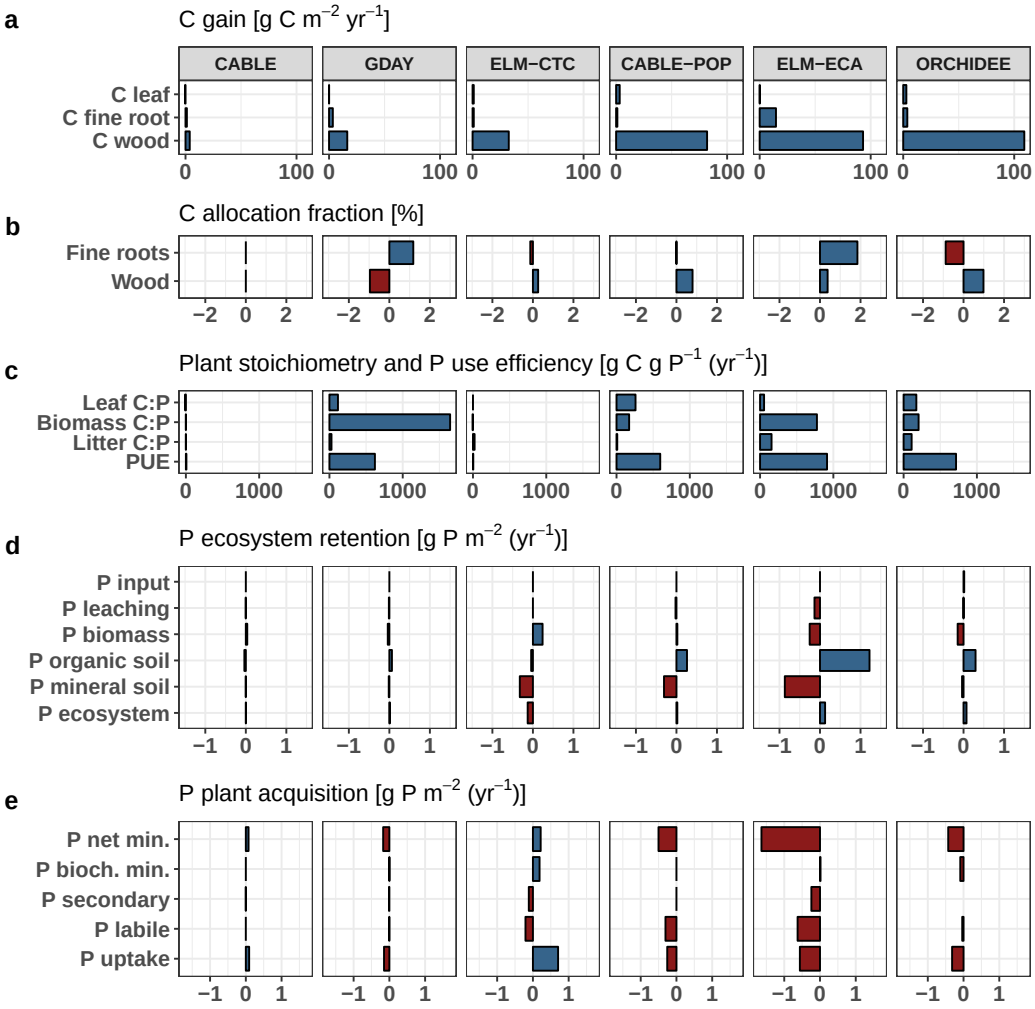

Figure 3: **Key responses of biomass C gain, stoichiometry, allocation, and P dynamics to eCO_2 for the CNP models**, contrasted are positive (blue) from negative (red) responses. **a**, Mean annual change in standing leaf, fine root and wood C over 15 years, increasing across models from left to right in g C m^{-2} yr^{-1}. **b**, The mean change in C allocation for fine roots and wood in %. **c**, Mean change in tissue stoichiometry in absolute terms in g C g P^{-1} and change in P use efficiency over 15 years in g C g P^{-1} yr^{-1}. **d**, Mean change in ecosystem P input and output (leaching) fluxes in g P m^{-2} yr^{-1} and mean change in final P stock in biomass, organic soil, mineral soil and total ecosystem in g P m^{-2}. **e**, Mean change in plant P acquisition processes, including change in net P mineralization, biochemical P mineralization and P uptake in g P m^{-2} yr^{-1} and secondary and labile P pools in g P m^{-2}. For both, **d** and **e**, P flux changes are differences of cumulative fluxes after 15 years and P pool changes are differences in pools after 15 years.